MOLECULAR AND CELLULAR BIOLOGY, Sept. 2007, p. 6532–6545 Vol. 27, No. 18
0270-7306/07/$08.00+0 doi:10.1128/MCB.00471-07

Mdt1 Facilitates Efficient Repair of Blocked DNA Double-Strand Breaks and Recombinational Maintenance of Telomeres▽

Brietta L. Pike[1]† and Jörg Heierhorst[1,2]*

St. Vincent's Institute of Medical Research[1] and Department of Medicine, St. Vincent's Hospital,[2] The University of Melbourne, Fitzroy, Victoria, Australia

Received 19 March 2007/Returned for modification 25 April 2007/Accepted 6 July 2007

DNA recombination plays critical roles in DNA repair and alternative telomere maintenance. Here we show that absence of the SQ/TQ cluster domain-containing protein Mdt1 (Ybl051c) renders *Saccharomyces cerevisiae* particularly hypersensitive to bleomycin, a drug that causes 3′-phospho-glycolate-blocked DNA double-strand breaks (DSBs). *mdt1*Δ also hypersensitizes partially recombination-defective cells to camptothecin-induced 3′-phospho-tyrosyl protein-blocked DSBs. Remarkably, whereas *mdt1*Δ cells are unable to restore broken chromosomes after bleomycin treatment, they efficiently repair "clean" endonuclease-generated DSBs. Epistasis analyses indicate that *MDT1* acts in the repair of bleomycin-induced DSBs by regulating the efficiency of the homologous recombination pathway as well as telomere-related functions of the KU complex. Moreover, *mdt1*Δ leads to severe synthetic growth defects with a deletion of the recombination facilitator and telomere-positioning factor gene *CTF18* already in the absence of exogenous DNA damage. Importantly, *mdt1*Δ causes a dramatic shift from the usually prevalent type II to the less-efficient type I pathway of recombinational telomere maintenance in the absence of telomerase in liquid senescence assays. As telomeres resemble protein-blocked DSBs, the results indicate that Mdt1 acts in a novel blocked-end-specific recombination pathway that is required for the efficiency of both drug-induced DSB repair and telomerase-independent telomere maintenance.

Maintenance of genome stability in eukaryotes depends on a range of lesion-specific DNA repair pathways that act in concert with checkpoint pathways, which attenuate cell cycle progression in the presence of unrepaired DNA damage (75). The importance of these pathways is underscored by findings that inherited mutations in numerous DNA repair and checkpoint-signaling genes are associated with cancer predisposition as well as aging-related disorders in humans (35, 75). DNA damage response pathways are remarkably conserved throughout evolution, which allows the efficient use of simple model organisms, such as budding yeast (*Saccharomyces cerevisiae*), to study fundamental aspects of DNA repair and damage signaling (75).

DNA double-strand breaks (DSBs) are widely considered to be the most dangerous form of DNA damage, and in yeast even a single unrepaired DSB is generally lethal (69). The preferred DSB repair pathway in yeast is the homologous recombination (HR) pathway, in which broken ends are repaired by a copy mechanism using homologous sequences as the template (18, 27). This mechanism is highly accurate when identical sister chromatids are available as templates but can be mutagenic or result in loss of heterozygosity when homologous chromosomes or nonallelic templates are copied (54). In order to invade homologous double-stranded templates, break ends have to be converted to extended single-stranded DNA (ssDNA) 3′ tails coated with the Rad51 recombinase (27). In haploid yeasts, conversion of DSBs into recombinogenic 3′ tails depends on cyclin B-dependent Cdc28 kinase activity, and DSBs can therefore only be repaired by HR after cell cycle Start in G_1, but DNA replication (or entry into S phase) is not necessary (2, 24). However, some other DNA lesions are repairable by HR before Start in haploid cells (24), and DSB repair by HR is also highly active before Start in diploid cells or haploid cells expressing an ectopic heterozygous mating type locus (70).

The main alternative for HR repair of DSBs throughout the cell cycle, and the preferred pathway before Start in haploid yeasts, is the nonhomologous end-joining (NHEJ) pathway (27). Because joining of broken ends involves some end processing, NHEJ is typically inaccurate and in the presence of multiple DSBs can even lead to chromosomal translocations. In budding yeast, DSB repair by NHEJ is much less efficient than by HR (18).

In *S. cerevisiae*, Rad51 loading onto ssDNA depends on Rad52, and in contrast to higher eukaryotes, yeast Rad52 can sustain some HR activity even in the absence of Rad51 (18, 27). Other recombination mediators that participate in aspects of HR biochemistry are Rad54, the Rad55-Rad57 complex, Rad59, and Rdh54, as well as the Mre11-Rad50-Xrs2 (MRX) complex (18, 27, 33). Because absence of *RAD52* abolishes all HR activity, it is widely used as the definitive marker gene for this pathway (27). NHEJ depends on the Yku70-Yku80 complex (KU) and DNA ligase 4, and the corresponding gene deletions are therefore often used as markers for the NHEJ pathway (61, 73). However, KU also functions in a third DSB repair pathway, chromosome "healing" that seals breaks by de novo telomerization (47, 57); as this leads to loss of the cen-

* Corresponding author. Mailing address: St. Vincent's Institute of Medical Research, 9 Princes Street, Fitzroy, VIC 3065, Australia. Phone: 61-3-9288-2503. Fax: 61-3-9416-2676. E-mail: jheierhorst@svi.edu.au.

† Present address: Friedrich Miescher Institute for Biomedical Research, Maulbeerstrasse 66, 4058 Basel, Switzerland.

▽ Published ahead of print on 16 July 2007.

tromere-distal fragment, this pathway can only sustain viability when no essential genes are located distal from the DSB. Likewise, Lig4 together with the MRX complex is required for an alternative poorly understood end-joining pathway that can repair microhomology-sharing DSB ends in the absence of Rad52 and KU (37).

In addition to the core proteins that participate directly in DSB repair biochemistry, a number of more indirectly acting recombination "facilitator" pathways have recently begun to emerge that are believed to be required for maximum efficiency of both HR and NHEJ pathways. These pathways include chromatin remodelling complexes (presumably to promote access of core repair components to break sites) (42, 56, 71), cohesins and cohesin-loading complexes (presumably to hold broken ends together until they are sealed) (9, 45, 67), and the proteasome (possibly to cleave damage-specific cohesins after successful repair) (26).

DNA repair pathways are complemented by checkpoints that delay the cell cycle in order to prevent cell division in the presence of damaged chromatin (75). Key enzymes in this process are the ATM/ATR-like checkpoint kinases Tel1 and Mec1 in yeast (55). While Mec1 is activated in response to a wide range of lesions that are converted to single-stranded DNA, e.g., 3′ tails resulting from DSBs, Tel1 activity is believed to be more restricted to the response to unprocessed DSBs (39, 68). Mec1 and Tel1 phosphorylate a large number of effectors, preferentially on SQ or TQ residues that are often concentrated in SQ/TQ cluster domains, in order to propagate the checkpoint signal (64). An important substrate is the Chk2-like protein kinase Rad53, which plays a crucial role in signal amplification and whose phosphorylation state is a widely used marker for general checkpoint activity (30, 46, 49, 50, 55). In case of very limited irreparable DNA damage (a single DSB in wild-type cells), checkpoint signals are eventually inactivated such that cells can adapt to persistent damage and resume proliferation until loss of the damaged chromosome leads to loss of viability (46). However, prompt DNA damage recovery after successful repair seems to be an active process that involves dephosphorylation of Mec1/Tel1 substrates by the protein phosphatases Ptc2/3 and Pph3 in order for cells to resume proliferation (25, 31). Some DNA repair proteins also contribute directly to checkpoint signaling; for example, Tel1 activation by unprocessed DSBs depends on the MRX complex (68), and checkpoint adaptation depends on KU (46).

Telomeres as the ends of linear chromosomes represent natural DSBs, and it is clear that there is extensive cross talk between DNA damage response and telomere maintenance pathways (10, 72). To distinguish chromosome ends from DSBs and prevent their illicit "repair," normal telomeres are hidden from the checkpoint and DNA repair machinery by a proteinaceous cap (10, 16, 72). Telomeres become progressively shorter with each cell cycle. Most organisms maintain telomere length using the specialized ribonucleoprotein complex telomerase that elongates chromosome ends by repetitive reverse transcription of a short template sequence from its RNA, resulting in uniform tandem repeat patterns at telomeres across the genome (72). DNA repair and checkpoint proteins play multiple, often seemingly contradictory functions in telomere biology. For example, although telomeres function to prevent NHEJ-dependent chromosome fusions (4), KU is part of the normal cap structure (3, 57), and while checkpoint kinases play important roles in facilitating telomerase access to shortening telomeres without causing a global checkpoint response (58), they elicit a general senescence signal when telomere repeats become critically short and chromosome ends become uncapped in the absence of telomerase (11). Interestingly, as a rare stochastic event, some cells regain the ability to maintain telomeres in the absence of telomerase and thereby escape senescence (29, 60). This formation of postsenescence type II survivors in yeast, or alternative lengthening of telomeres in human cancer cells (43), involves recombinational telomere elongation using other telomere repeats as templates, possibly in the form of extrachromosomal telomere circles (17, 28, 32). In addition, yeast cells can utilize another less-efficient recombination pathway that involves subtelomeric template sequences to form so-called type I survivors (6, 60), and a similar mechanism may also exist in human cells (13). Although a number of genes have been identified that are required for formation of type I or type II survivors, the mechanisms that regulate the choice between these pathways remain largely unclear.

We recently identified the SQ/TQ cluster domain-containing protein Mdt1 as a novel Mec1/Tel1 substrate and Rad53-interacting protein in yeast (51). *mdt1* deletion mutants have an elongated cell morphology and a noticeable G_2/M cell cycle delay under basal conditions, a phenotype often found in DNA damage response-defective mutants. Surprisingly, *mdt1*Δ modestly suppressed the methylmethane sulfonate (MMS) hypersensitivity of some checkpoint mutants, which may in part be due to its slower G_2/M transition. In order to better understand the DNA damage response functions of Mdt1, we sought to identify DNA lesions to which *mdt1*Δ mutants are hypersensitive rather than partially resistant. Here we show that *mdt1*Δ cells are highly sensitive to bleomycin, a glycopeptide antibiotic that causes blocked DSBs (5, 53), and we also show that *mdt1*Δ affects the efficiency of recombinational telomere maintenance. Because Mdt1 seems to specifically affect blocked drug-induced DSBs, but not clean endonuclease-induced DSBs, and because telomeres due to their proteinaceous cap in a way resemble blocked DNA ends, our results suggest that Mdt1 may be involved in a blocked-end-specific recombination pathway.

MATERIALS AND METHODS

Yeast strains. The yeast strains used are listed in Table 1. Unless stated otherwise, experiments were performed in the W303-1a background with corrected *RAD5*, kindly provided by Rodney Rothstein (74), and in most cases containing a deletion of *SML1* in order to prevent indirect suppression of DNA damage hypersensitivity from elevated deoxynucleoside triphosphate levels (8, 74). In some crosses and sporulations, *MDT1-1 MYC* and *MDT1-13 MYC-KAN* alleles were used as wild type (Table 1), and where this was done relevant controls showed that they behaved similarly to *MDT1* in DNA damage sensitivity or telomere maintenance assays. The 10x*TY-HO* strain kindly provided by Lorraine Symington is in the same W303-1a background (34). Additional HO endonuclease-induced DSB experiments were performed in the JKM179 (46) and TGI354 (23) strain background kindly provided by Jim Haber. Interaction analyses with *smc5* alleles (9) kindly provided by Greg Cost were performed in the S288c (BY4741) background after sporulation of diploid crosses with *mdt1*Δ in an isogenic *MFA1pr-HIS3* strain kindly provided by Brenda Andrews (63). All gene disruptions shown in the table are PCR-based deletions of the entire relevant open reading frame as described before (51). Unless stated otherwise, all experiments were performed using YPD (1% yeast extract, 2% peptone, 2% glucose) at 30°C.

TABLE 1. Yeast strains used in this study

Strain	Relevant genotype[a]	Background	Source
Y52	*MAT***a** *ade2-1 can1-100 leu2-3,112 trp1-1 ura3-1 RAD5*	W303-1a	74
Y53	*sml1*::*HIS3*	W303-1a	74
Y189	*MDT1-1 MYC sml1*::*HIS3*	W303-1a	51
Y400	*MDT1-13 MYC-KAN sml1*::*HIS3*	W303-1a	
Y109	*mdt1*::*LEU2 sml1*::*HIS3*	W303-1a	51
Y330	*mdt1*::*KAN sml1*::*HIS3*	W303-1a	
Y470	*mdt1*::*klURA3 sml1*::*HIS3*	W303-1a	
Y208	*MDT1-1 MYC mec1*::*klURA3 sml1*::*HIS3*	W303-1a	51
Y341	*mec1*::*klURA mdt1*::*LEU2 sml1*::*HIS3*	W303-1a	
Y275	*MDT1-1 MYC tel1*::*klURA3 sml1*::*HIS3*	W303-1a	
Y386	*mdt1*::*LEU2 tel1*::*NAT sml1*::*HIS3*	W303-1a	
Y392	*rad52*::*NAT MDT1-MYC sml1*::*HIS3*	W303-1a	
Y393	*rad52*::*NAT mdt1*::*LEU2 sml1*::*HIS3*	W303-1a	
Y399	*yku70*::*klURA3 MDT1-13 MYC-KAN sml1*::*HIS3*	W303-1a	
Y406	*yku70*::*klURA3 mdt1*::*LEU2 sml1*::*HIS3*	W303-1a	
Y402	*yku70*::*klURA3 rad52*::*NAT MDT1-13MYC-KAN sml1*::*HIS3*	W303-1a	
Y404	*yku70*::*klURA3 rad52*::*NAT mdt1*::*LEU2 sml1*::*HIS3*	W303-1a	
Y411	*RAD52/rad52*::*NAT YKU70/yku70*::*klURA3 MDT1-13 MYC-KAN/mdt1*::*LEU2 SML1/sml1*::*HIS3*	W303 diploid	
Y578	*ctf18*::*NAT/CTF18 mdt1*::*LEU2/MDT1 sml1*::*HIS3/sml1*::*HIS3*	W303 diploid	
Y480	*sem1*::*klURA3/SEM1 mdt1*::*LEU2/MDT1-13 MYC-KAN sml1*::*HIS3/sml1*::*HIS*	W303 diploid	
Y494	*arp5*::*klURA3/ARP5 MDT1-13 MYC-KAN/mdt1*::*LEU2*	W303 diploid	
Y395	*MDT1-13 MYC-KAN rad50*::*NAT sml1*::*HIS*	W303-1a	
Y445	*rad50*::*NAT mdt1*::*LEU2 sml1*::*HIS*	W303-1a	
Y440	*MDT1-13 MYC-KAN rad51*::*NAT sml1*::*HIS*	W303-1a	
Y447	*rad51*::*NAT mdt1*::*LEU2 sml1*::*HIS*	W303-1a	
Y443	*MDT1-13 MYC-KAN rad55*::*NAT SML1*	W303-1a	
Y451	*rad55*::*NAT mdt1*::*LEU2 SML1*	W303-1a	
Y365	*est2*::*KAN/EST2 MDT1-MYC/mdt1*::*LEU2 sml1*::*HIS3/SML1*	W303 diploid	
Y415	*MDT1-1 MYC/mdt1*::*LEU rad52*::*NAT/RAD52 est2*::*KAN/EST2 sml1*::*HIS3/sml1*::*HIS3*	W303 diploid	
Y429	LSY1248 10xTy-HO	W303-1a	34
Y430	LSY1248 10xTy-HO mdt1::*KAN*	W303-1a	
Y433	LSY1248 10xTy-HO rad52::*NAT*	W303-1a	
Y434	LSY1248 10xTy-HO mdt1::*KAN rad52*::*NAT*	W303-1a	
Y219	*ho*Δ *hml*Δ::*ADE1 hmr*Δ::*ADE1 ade3*::*GAL10*::*HO MAT*α	JKM179	46
Y225	Y219 *sml1*::*KAN*	JKM179	46
Y286	Y219 *mdt1*::*klURA3 sml1*::*KAN*	JKM179	
Y496	*ho hml*::*ADE2 MAT***a**-inc *hmr*::*ADE1 ade1 leu2-3,112 lys5 trp1*::*hisG ura3-52 ade3*::*GAL*::*HO arg5,6*::*MAT***a**::*HPH*	TGI354	23
Y505	Y496 *mdt1*::*KAN*	TGI354	
Y507	Y496 *rad52*::*NAT*	TGI354	
Y542	Y496 *rad52*::*NAT mdt1*::*LEU2*	TGI354	
Y557	Y496 *yku70*::*NAT*	TGI354	
Y619	Y496 *yku70*::*NAT mdt1*::*KAN*	TGI354	
Y588	UCC3505 *URA3-TEL-VII-L VR-ADE-TEL*	YPH499	57
Y590	Y588 *yku80*::*KanMX*	YPH499	57
Y593	Y588 *mdt1*::*NAT*	YPH499	
Y594	Y588 *yku80*::*KanMX mdt1*::*NAT*	YPH499	
Y372	Y5565 MATα *can1*Δ::*MFA1pr-HIS3 mf*α*1*Δ::*MF*α*1pr-LEU2 lyp1*Δ *HIS3*Δ*1 LEU2*Δ*0 ura3*Δ*0met15*Δ*0 LYS2*$^+$	S288c	63
Y373	Y372 *mdt1*::*NAT*	S288c	
Y499	*MAT***a** *smc5*::*kanMX4 his3*Δ*1 leu2*Δ*0 lys2*Δ*0 met15*Δ*0 ura3*Δ*0* [*pGC251-LEU2 SMC5*]	S288c	9
Y500	*MAT***a** *smc5*::*kanMX4 his3*Δ*1 leu2*Δ*0 lys2*Δ*0 met15*Δ*0 ura3*Δ*0* [*pGC251-LEU2 smc5-31*]	S288c	9
Y501	*MAT***a** *smc5*::*kanMX4 his3*Δ*1 leu2*Δ*0 lys2*Δ*0 met15*Δ*0 ura3*Δ*0* [*pGC251-LEU2 smc5-33*]	S288c	9
Y522	*MAT***a** *p-SMC5*	S288c	
Y523	*MAT***a** *p-SMC5 mdt1*::*NAT*	S288c	
Y524	*MAT***a** *p-smc5-31*	S288c	
Y525	*MAT***a** *p-smc5-31 mdt1*::*NAT*	S288c	
Y526	*MAT***a** *p-smc5-33*	S288c	
Y527	*MAT***a** *p-smc5-33 mdt1*::*NAT*	S288c	

[a] Only genotypes that differ from the relevant parental background strain are indicated, and unless otherwise noted haploid strains are *MAT***a**. For clarity, strains are ordered by experimental context rather than number. Unless otherwise noted, strains were newly generated for this study.

DNA damage sensitivity assays. For liquid survival assays, overnight cultures were diluted to an A_{600} of 0.2 and grown for 3 h before removal of an undamaged control aliquot and addition of bleomycin at the indicated doses for 4 h, followed by plating of relevant dilutions onto fresh YPD plates and counting of colonies after 3 to 4 days. Survival is the fraction of colonies formed at the indicated doses compared to the untreated control. Data shown in the figures are the means ± standard errors of six or more independent experiments. Results shown here were obtained with three different batches of bleocin (Calbiochem), and similar effects albeit at higher doses were also observed using bleomycin from Sigma and the structurally related compounds zeocin (Invitrogen) and phleomycin (Calbiochem). For drop test assays, log-phase cultures were diluted to an A_{600} of 0.05, and serial 10-fold dilutions were plated on YPD, YPD containing 20 ng/ml bleomycin, 0.5 μg/ml camptothecin, and 0.0025% MMS or on YPSG (1% yeast extract, 2% peptone, 2% sucrose, 2% galactose) for *GAL1-HO* induction. For *GAL1-HO* induction in liquid cultures, cells were pregrown in 2% raffinose for 1 to 2 days before addition of 2% galactose for the indicated times.

Protein and nucleic acid blot assays. For Northern and Western blot assays, samples were treated using 0.5 μg/ml bleomycin or 100 mM hydroxyurea for 2 h, unless stated otherwise in the figures or legends. For Western blot assays, lysates were prepared using glass beads and urea buffer and subjected to 8% sodium dodecyl sulfate-polyacrylamide gel electrophoresis, transferred onto a polyvinylidene difluoride membrane, and detected with a rabbit anti-Rad53-FHA1 antibody as described elsewhere (48). DNA and RNA were prepared using glass beads and phenol-$CHCl_3$ extraction, and blots were probed under high-stringency conditions using [α-^{32}P]dCTP-labeled cDNAs followed by exposure to PhosphorImager screens (Molecular Dynamics) as described previously (49, 50). In all cases, ~500-bp gene-specific probes were amplified by PCR, cloned into pGEM-T, confirmed by sequencing, and gel purified after restriction endonuclease digestion before labeling. Telomere blots were probed using a Y′-probe.

PFGE. Cells were treated with 10 μg/ml bleomycin for 2 h, washed, and released into YPD for up to 5 h. Aliquots removed before and immediately following bleomycin treatment, and at various recovery time points, were embedded in low-melting-point agarose for preparation of high-molecular-weight DNA and pulsed-field gel electrophoresis (PFGE) using GE Healthcare Gene Navigator equipment following routine procedures. Gels were stained using 0.5 μg/ml ethidium bromide and transferred for Southern blot analysis using 18S rDNA (chromosome XII) and *RNR2* (chromosome X) probes as described previously (19).

Tetrad analyses and senescence assays. Sporulation cultures were digested using zymolyase 20T in sorbitol buffer, and tetrads were dissected on YPD plates using a Singer yeast dissection microscope. Photographs of plates were taken after 2 to 3 days, and colonies were genotyped by plating of aliquots onto selective plates for the relevant gene deletion markers (Table 1) or by PCR. For senescence assays, larger colonies were transferred into 200 μl 1 M sorbitol after 2 days, while smaller colonies were transferred after 3 days to normalize generation numbers, and kept at 4°C until genotyping was complete. Fifty-μl aliquots of cells were then transferred to 10 ml YPD, and in 24-hour intervals hemocytometer counted and diluted to 10^5 cells/ml. In addition, each day 100 to 200 cells were plated on YPD, and colonies were counted after 3 to 4 days. DNA was prepared from aliquots of day 1 liquid cultures for terminal restriction fragment analyses of presenescent cells and from day 8 liquid cultures as well randomly selected survivor colonies from day 8 plates for analyses of postsenescent cells. In addition, DNA was also prepared from survivor colonies grown in liquid for another 6 days.

Telomere position effect. Subtelomeric gene silencing assays were performed in *URA3-TEL-VII-L* reporter strains in the YPH499 background (57) kindly provided by Dan Gottschling by plating on 5-fluoroorotic acid (FOA).

RESULTS

Mdt1 is required for bleomycin survival in a largely checkpoint-independent manner. While screening a range of DNA-damaging agents, we found that *mdt1*Δ mutants were exquisitely hypersensitive to the DSB-inducing drug bleomycin (Fig. 1A) but not to several other genotoxic agents (e.g., MMS, HU, mitomycin C, UV, H_2O_2, and etoposide [data not shown]), with ~100-fold-reduced survival compared to the wild type after acute drug exposure for 4 h (Fig. 1A). This phenotype was observed by using several different selectable markers for deletion of *MDT1* (Table 1), it segregated with *mdt1*Δ in tetrad dissections, and it could be complemented by plasmid-borne *MDT1* (data not shown).

Because Mdt1 is a Mec1/Tel1 substrate (51), we compared its role in the bleomycin response to the checkpoint machinery. Interestingly, *mdt1*Δ cells were even more bleomycin hypersensitive than checkpoint-defective *mec1*Δ cells (Fig. 1A), but *mec1*Δ *mdt1*Δ double mutants were considerably more hypersensitive than the single mutants (Fig. 1A). This dramatic synthetic effect demonstrates that Mdt1 acts in a separate pathway from Mec1 in the bleomycin response.

*tel1*Δ had only very mild bleomycin hypersensitivity and, surprisingly, even slightly suppressed the *mdt1*Δ phenotype (Fig. 1A). However, *tel1*Δ *mdt1*Δ double mutants were still very highly bleomycin hypersensitive (i.e., as much as *mec1*Δ) (Fig. 1A), indicating that although hyperactivation of a Tel1-specific checkpoint (see below) could be a contributing factor, it is not a major reason for the impaired colony formation of *mdt1*Δ cells after bleomycin treatment.

An important checkpoint effector pathway for survival of DNA damage involves transcriptional induction of DNA repair genes (75). However, four of the most strongly DNA damage-inducible genes (*RNR3*, *RAD54*, *HUG1*, and *GTT2*) were expressed at normal levels in *mdt1*Δ cells (Fig. 1B), indicating that *mdt1*Δ bleomycin hypersensitivity is not caused by defective transcriptional responses to DNA damage.

***mdt1*Δ impairs checkpoint recovery after bleomycin treatment.** In parallel with the genetic analyses, we directly monitored checkpoint activity by immunoblot analysis of DNA damage-induced phosphorylation-dependent mobility shifts of the key Mec1/Tel1 substrate Rad53. Consistent with the notion that Mec1 is the more "dominant" of these kinases (55), and proportional to their relative bleomycin hypersensitivities (Fig. 1A), bleomycin-induced Rad53 mobility shifts were almost completely abolished in *mec1*Δ cells (Fig. 1C, lane 6) but undiminished in the absence of Tel1 (Fig. 1C, compare lanes 2 and 10). Interestingly, *mdt1*Δ led to noticeably increased Rad53 shifts in otherwise-wild-type cells (Fig. 1C, compare lanes 2 and 4) and *tel1*Δ mutants (Fig. 1C, compare lanes 10 and 12). Moreover, *mdt1*Δ partially suppressed the Rad53 phosphorylation defect of *mec1*Δ cells (Fig. 1C, compare lanes 6 and 8). The Mec1-independent restoration of Rad53 phosphorylation by *mdt1*Δ was quite striking, as improved checkpoint competence would normally be expected to coincide with improved bleomycin survival, yet paradoxically, deletion of *MDT1* dramatically worsened bleomycin tolerance of *mec1*Δ mutants (Fig. 1A).

More detailed time course analyses indicated that Rad53 phosphorylation following bleomycin addition was not accelerated in *mdt1*Δ cells (Fig. 1D), but rather that the reversal of Rad53 shifts upon bleomycin removal was clearly delayed in the absence of Mdt1: whereas Rad53 shifts were gradually reversed in the wild type with full restoration of basal mobility within 4 h, Rad53 shifts were only partially reversed in the mutant even after 5 h (Fig. 1E). Remarkably, at the 5-hour time point the Rad53 banding pattern in *mdt1*Δ was very similar to the 1-hour time point in the wild type. Altogether, these time course experiments demonstrate that the net increase in Rad53 mobility shifts in *mdt1*Δ cells after 2-hour bleomycin treatment (Fig. 1C) is primarily due to delayed Rad53 inacti-

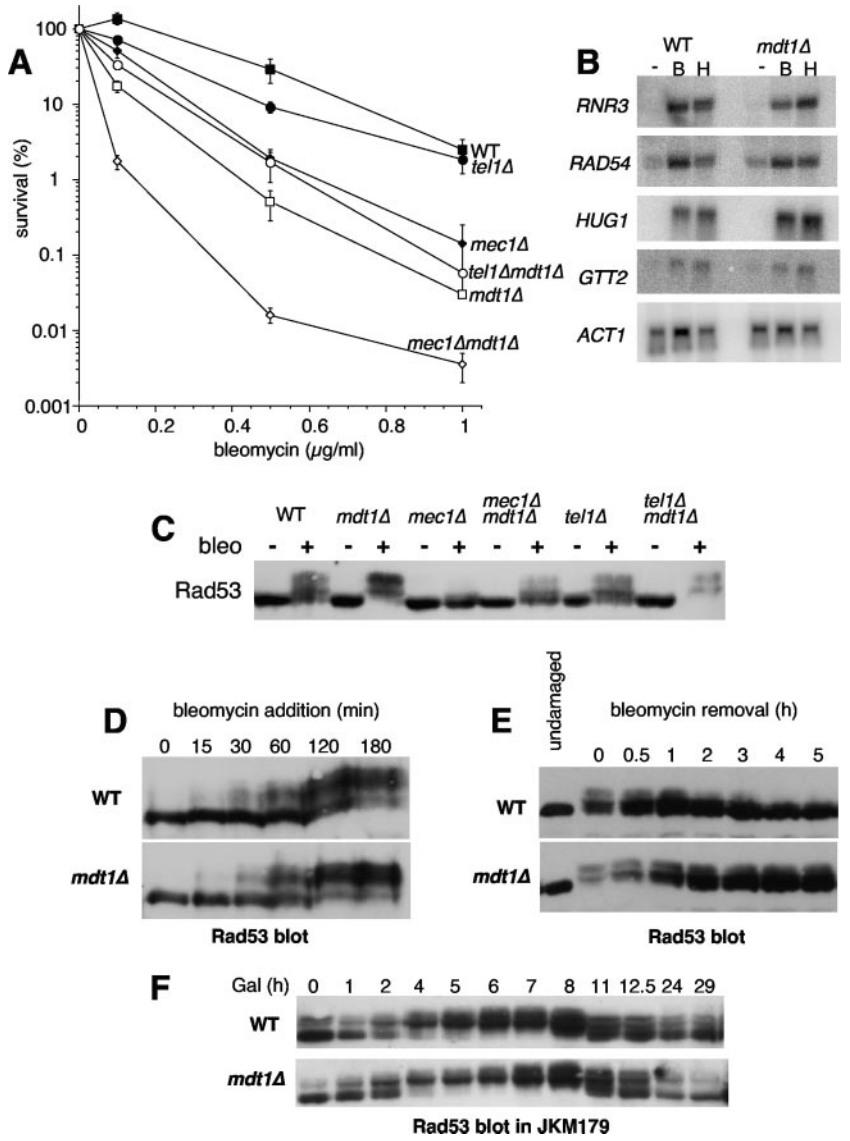

FIG. 1. DNA damage checkpoint interactions of *MDT1* in the bleomycin response. (A) Bleomycin survival dose-response curves of the indicated yeast strains. Data are means ± standard errors. WT, wild type. (B) Northern blot analysis of the indicated gene transcripts from untreated (−) or bleomycin (B)- or hydroxyurea (H)-treated wild-type or *mdt1*Δ cells. (C) Rad53 immunoblot analysis of the indicated strains without (−) or after (+) bleomycin treatment. (D) Rad53 immunoblot analysis of wild-type or *mdt1*Δ cells at the indicated times after bleomycin addition. (E) Rad53 immunoblot analysis of untreated wild-type and *mdt1*Δ cells at the indicated times after release from bleomycin treatment for 2 h. (F) Rad53 immunoblot analysis of JKM149 or its *mdt1*Δ derivative at the indicated time points (hours) after galactose addition to induce a single irreparable DSB.

vation, indicating that Mdt1 is required for efficient checkpoint recovery from bleomycin-induced DNA damage.

In contrast to the bleomycin recovery defect, *mdt1*Δ had no effect on Rad53 inactivation kinetics in the adaptation to a single unrepairable (galactose-induced) HO endonuclease-generated DSB in the JKM179 strain (although there was some leaky *GAL1-HO* expression, the timing and extent of Rad53 shifts after galactose addition were very similar in wild-type and *mdt1*Δ cells with maximal Rad53 shifts between 4 and 8 h and adaptation from about 11 h [Fig. 1F]). Furthermore, we did not observe any Rad53 hyperactivation in *mdt1*Δ mutants in response to MMS or HU (51) (data not shown). These results demonstrate that, in principle, Rad53 activation can be efficiently reversed in *mdt1*Δ mutants (even if the damage persists), indicating that their recovery defect is quite lesion specific for the bleomycin response.

***mdt1*Δ bleomycin hypersensitivity is epistatic with compound DSB repair deficiency.** Given that impaired Rad53 dephosphorylation did not seem to be the primary cause of the bleomycin recovery defect, the most plausible explanation for persistent checkpoint signals in *mdt1*Δ mutants was impaired DNA damage processing and repair. Furthermore, as the only way to activate Rad53 in the absence of Mec1 is via Tel1, and as Tel1 is believed to be preferentially activated by unprocessed DSBs (68), the restored phosphorylation of Rad53 in *mec1*Δ *mdt1*Δ double mutants (Fig. 1C) prompted us to assess

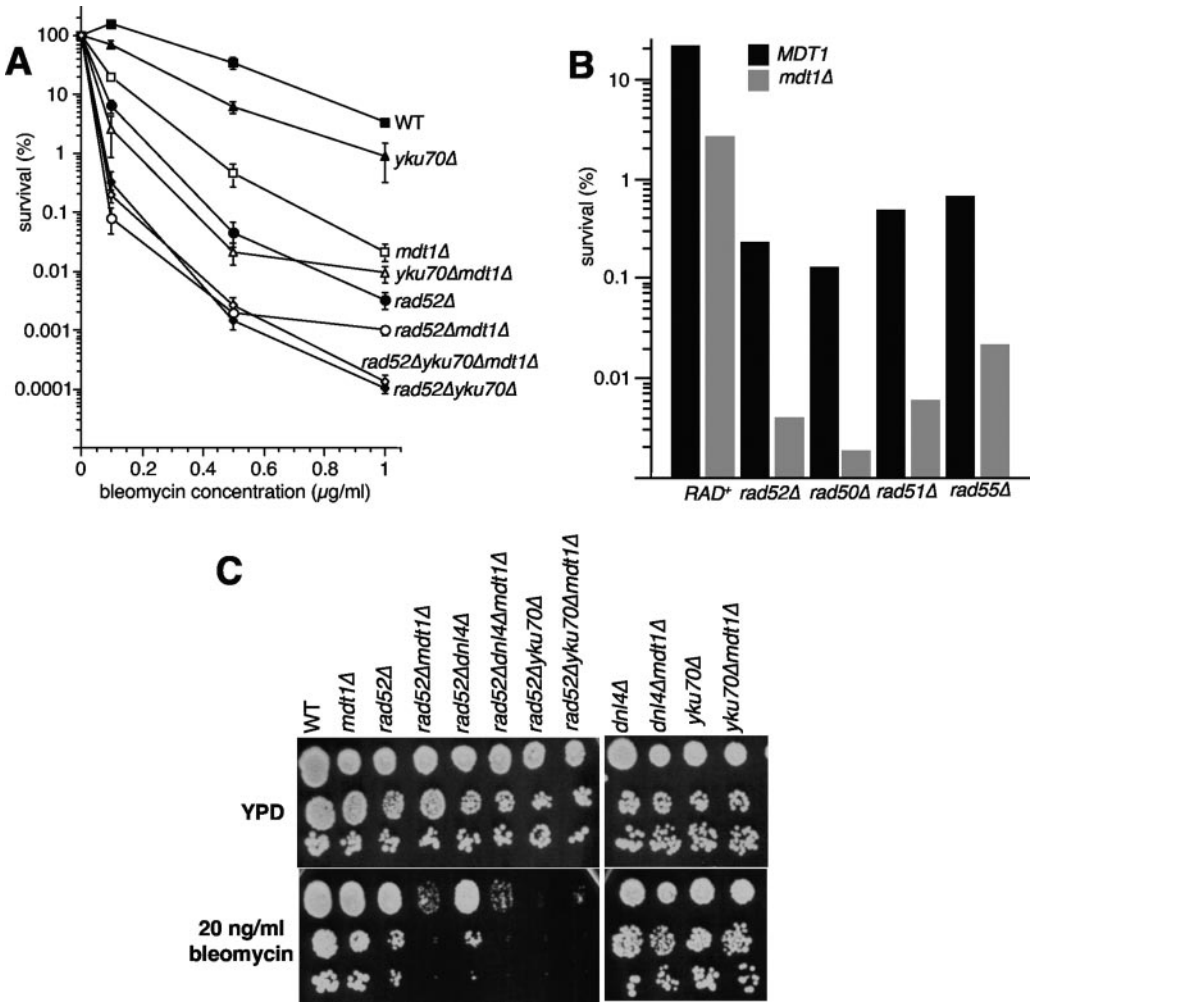

FIG. 2. DSB repair pathway interactions of *MDT1* in the bleomycin response. (A) Interactions with *rad52*Δ and *yku70*Δ. Data are the means ± standard errors of bleomycin survival dose responses of the indicated strains at the indicated doses of bleomycin for 4 h. (B) Interactions with selected members of the *RAD52* epistasis group. Data are the averages of duplicate cultures treated with 0.5 μg/ml bleomycin for 4 h. (C) Drop test analysis of serial 10-fold dilutions of the indicated strains on YPD or YPD plus 20 ng/ml bleomycin plates.

possible roles of Mdt1 in the repair of bleomycin-induced DSBs.

DSBs as the major cytotoxic lesions caused by bleomycin are preferably repaired by HR (18), and consequently, HR-deficient *rad52*Δ cells were very highly bleomycin sensitive (~10-fold more than *mdt1*Δ) over a range of doses (Fig. 2A). However, *rad52*Δ *mdt1*Δ double mutants were another order of magnitude more sensitive to bleomycin than *rad52*Δ alone (Fig. 2A), indicating that *MDT1* has at least some *RAD52*-independent functions, and similar synthetic genetic interactions were observed with other members of the *RAD52* epistasis group (Fig. 2B). We therefore analyzed *mdt1*Δ for interactions with the KU complex that is required for the main alternatives to HR-dependent DSB repair, NHEJ and chromosome healing by de novo telomere addition (27). *yku70*Δ alone had only a very modest bleomycin sensitivity but markedly increased the bleomycin hypersensitivity of *mdt1*Δ cells to levels similar to that of *rad52*Δ mutants (Fig. 2A), indicating that Mdt1 also has KU-independent functions. However, *mdt1*Δ had no synthetic effect on *rad52*Δ *yku70*Δ double mutants, which are essentially unable to repair DSBs and that were therefore ~10-fold more bleomycin hypersensitive than *rad52*Δ alone (Fig. 2A). We have recently reported that KU acts in the bleomycin response largely via telomere-related, NHEJ-independent functions (59). Consistent with this, we found here that in contrast to *rad52*Δ *yku70*Δ (which affects HR, NHEJ, and de novo telomere addition) *mdt1*Δ considerably worsened *rad52*Δ *dnl4*Δ (which affects all of the above except de novo telomere addition) bleomycin sensitivity (Fig. 2C). Furthermore, in contrast to *yku70*Δ (Fig. 2A and C), *dnl4*Δ did not worsen the phenotype of *rad52*Δ *mdt1*Δ (Fig. 2C), indicating that Mdt1 seems to act here in concert with telomere- but not NHEJ-related functions of KU. Bleomycin sensitivity in yeast is regulated by a number of DNA repair-independent pathways, and it also causes a range of single-stranded lesions that can be cytotoxic if not properly repaired (53). If Mdt1 acted in any of these pathways, or if it increased bleomycin uptake or delayed bleomycin detoxification, it should have resulted in a higher number of cytotoxic lesions and caused a left shift of the survival curve in *rad52*Δ *yku70*Δ

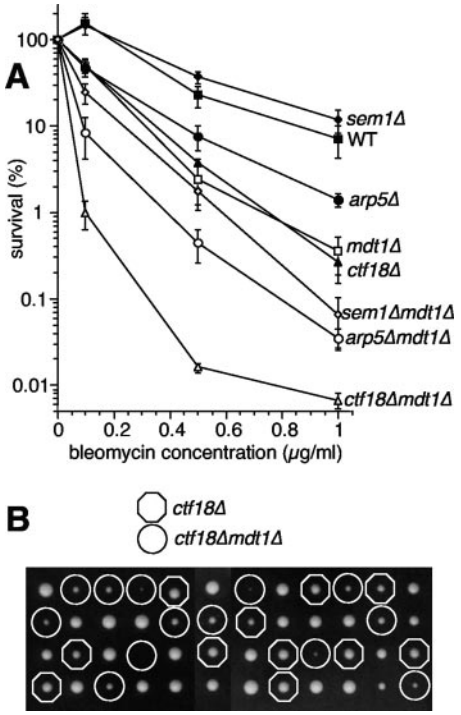

FIG. 3. *MDT1* interactions with recombination facilitators. (A) Bleomycin survival dose-response curves for the indicated strains (mean ± standard error). (B) Tetrad analysis of *CTF18*/*ctf18*Δ and *MDT1*/*mdt1*Δ on a YPD plate. Octagons indicate *ctf18*Δ single mutants, and circles indicate *ctf18*Δ *mdt1*Δ double mutants. Note that double mutant spores generally result in smaller colonies than *ctf18*Δ with no obvious growth defects for *mdt1*Δ compared to the wild type.

*mdt1*Δ triple mutants relative to *rad52*Δ *yku70*Δ double mutants. The epistatic relationship of *mdt1*Δ with the *rad52*Δ *yku70*Δ double mutation (but not *rad52*Δ *dnl4*Δ) therefore provides the strongest possible genetic evidence for a role of Mdt1 in the repair of bleomycin-induced DSBs that seems to involve both the HR pathway and telomere-related functions of KU.

***mdt1*Δ leads to reduced genetic fitness in the absence of the *CTF18* recombination facilitator.** The finding that *mdt1*Δ was epistatic with *rad52*Δ *yku70*Δ, but synthetic with both *rad52*Δ or *yku70*Δ single mutations (Fig. 2), indicates that Mdt1 is required for maximum efficiency of both the HR and the KU pathways in the repair of bleomycin-induced DSBs, reminiscent of a potential recombination facilitator function. We therefore compared *mdt1*Δ bleomycin hypersensitivity to deletions of representative nonessential genes of three separate facilitator pathways, the proteasome (*sem1*Δ) (26), the Ino80 chromatin remodelling complex (*arp5*Δ) (71), and a cohesin loading complex (*ctf18*Δ) (20). *mdt1*Δ bleomycin hypersensitivity was more severe than that of *sem1*Δ and *arp5*Δ mutants, and in both cases combination with *mdt1*Δ increased the phenotype (Fig. 3A). Interestingly, bleomycin hypersensitivity was very similar among *mdt1*Δ and *ctf18*Δ single mutants, but double deletion again led to a very dramatic potentiating effect (Fig. 3A). Moreover, during tetrad dissections to generate these strains, we noted that *ctf18*Δ *mdt1*Δ double mutants had a very strong synthetic "sickness" phenotype already in the absence of exogenous DNA-damaging agents (Fig. 3B).

In comprehensive genome-wide synthetic genetic interaction screens, *ctf18*Δ is relatively promiscuous with some 60 or so synthetic lethal or synthetic sick interactions in similar noncompetitive growth assays (63). Interestingly, the vast majority of these *CTF18*-interacting genes have established roles in DNA replication, recombination, or repair (63). The strong basal genetic interaction with *CTF18* (Fig. 3B) therefore provides reasonable indirect evidence for a role of *MDT1* in maintaining genome integrity in response to drug-independent physiological DNA lesions, although synergistic increases in bleomycin hypersensitivity place *MDT1* in a separate pathway from the recombination facilitators analyzed here (Fig. 3A).

Mdt1 is required for restoration of bleomycin-damaged chromosomes. Although bleomycin as a glycopeptide endonuclease has some sequence specificity, it is likely to cause DSBs in a fairly random fashion. To directly test the hypothesis that Mdt1 affects repair of bleomycin-induced DSBs, we therefore monitored the repair of bleomycin-broken chromosomes by PFGE. High-dose bleomycin treatment led to disappearance of intact chromosomes as visualized by ethidium bromide staining and chromosome-specific Southern blot analysis of pulsed-field gels (Fig. 4). In wild-type cells, intact chromosomes were restored by about 1 hour after bleomycin removal for chromosome X and at later time points for the largest chromosome XII (Fig. 4). The delayed repair of chromosome XII compared to chromosome X is consistent with the expected random distribution of bleomycin-induced DSBs, whereby larger chromosomes are more likely to be hit and as a result of more breaks then take proportionally longer to be repaired. Remarkably, absolutely no restored chromosomes—even in case of the relatively rapidly repaired chromosome X—were observed in the *mdt1*Δ mutant (Fig. 4). Interestingly, whereas high-molecular-weight putative repair intermediates (DSB repair by HR involves strand invasion between sister chromatids, resulting in atypical "cruciform" structures with retarded electrophoretic mobility) that did not properly enter the gel were detectable in the wild type, these were absent in *mdt1*Δ cells (Fig. 4), indicating that repair of bleomycin-induced DSBs may be blocked in *mdt1*Δ at a very early stage. Bleomycin seemingly induced slightly more damage in *mdt1*Δ than in the wild type; however, considering that repair does not just start after release into bleomycin-free medium but competes with damage throughout the experiment in repair-competent cells, this is exactly what would be expected after some time of continuous DNA damage in repair-deficient cells. Altogether, these results therefore support the genetic analyses (Fig. 2A) and Rad53 activation kinetics (Fig. 1D and E) that *mdt1*Δ cells are impaired in the repair of bleomycin-induced DSBs.

Mdt1 is not required for the repair of "clean" endonuclease-generated DSBs. To test if Mdt1 has general functions in DSB repair beyond the response to drug-induced DNA lesions, we analyzed its role in response to a single repairable endonuclease-generated DSB. For this purpose, we utilized the TGi354 strain (23), where an HO-induced DSB at an ectopic *MAT* sequence on chromosome V can only be repaired by HR when a modified HO-resistant *MAT***a**-inc template at the natural chromosome III locus is used as the template (Fig. 5A). Be-

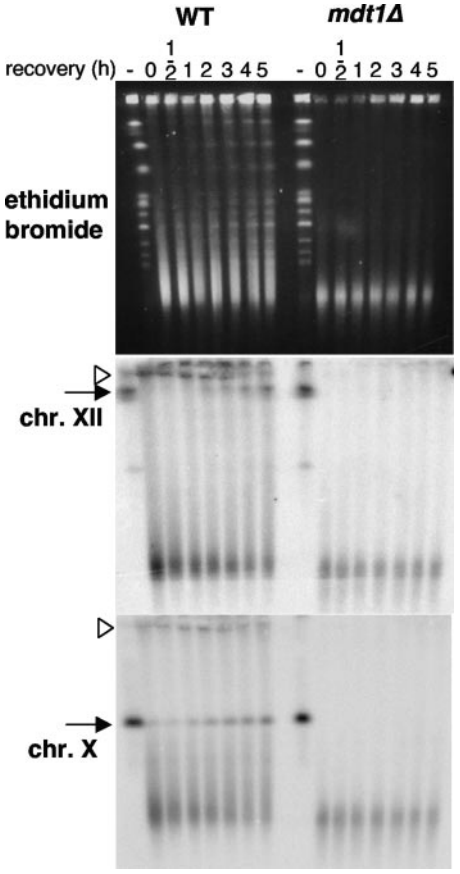

FIG. 4. Pulsed-field gel electrophoretic analysis of bleomycin damage repair. Cells were treated with 10 μg/ml bleomycin for 2 h and released into YPD. DNA before (-) and at the indicated times after bleomycin removal was analyzed in 1.2% agarose using 0.5× Tris-borate-EDTA buffer at 8°C with 90-s, 105-s, and 120-s pulses of 170 V, 100 mA, 100 W for 8 h each, before ethidium bromide staining (top) and Southern blot analyses for chromosomes XII (middle) and X (bottom). Arrow, intact chromosome; arrowhead, putative repair intermediate.

cause the DSB is repaired by the *MAT***a**-inc sequence, HO can only cut once, even if it is continuously expressed from the *GAL1* promoter. In this strain, continuous HO expression for 3 days is well tolerated by wild-type cells, but due to the inefficiency of NHEJ in yeast, less than 1% of *rad52*Δ cells survive HO expression (Fig. 5B), as expected. However, *mdt1*Δ did not affect cell survival in this assay (Fig. 5B). This lack of a gross survival defect was not due to reduced HO expression or reduced cleavage efficiency, because *mdt1*Δ did not suppress the *rad52*Δ phenotype (Fig. 5B). To determine if *mdt1*Δ had a more subtle DSB repair defect that may not be detectable in a 3-day survival assay, we directly measured repair of the HO-induced break by Southern blot analysis. Figure 5C shows that galactose addition led to efficient DSB formation at the ectopic *MAT* locus on chromosome V (but not *MAT***a**-inc on chromosome III; see figure insert) and that this break was then repaired with similar efficiency in *mdt1*Δ cells as in the wild type. In contrast to the strong synthetic interaction between *yku70*Δ and *mdt1*Δ for bleomycin tolerance (Fig. 2), even *yku70*Δ *mdt1*Δ double mutants were able to efficiently repair the HO-induced DSB (Fig. 5C). Therefore, contrary to the genetic evidence (Fig. 2) and whole-chromosome analyses (Fig. 4) that link *MDT1* to roles in repair of bleomycin-induced DSBs, *MDT1* seems to be dispensable for repair of a defined endonuclease-generated DSB at an ectopic mating type locus.

Two possible explanations for this discrepancy were that DSB repair at the *MAT* locus may be epigenetically different from random DSBs elsewhere in the genome, because this is how yeast change their mating type when they need to (with the caveat that in this case the DSB is in an ectopic location), and DSB repair at *MAT* is therefore a somewhat routine event, or that Mdt1 may only be required for repair in the presence of multiple simultaneous DSBs as caused by higher drug doses but not in the single-break assay (again, with the caveat that if a single DSB is already lethal in *rad52*Δ, its bleomycin sensitivity should not be increased by *mdt1*Δ). To address these possibilities, we performed similar *GAL1-HO* experiments in a

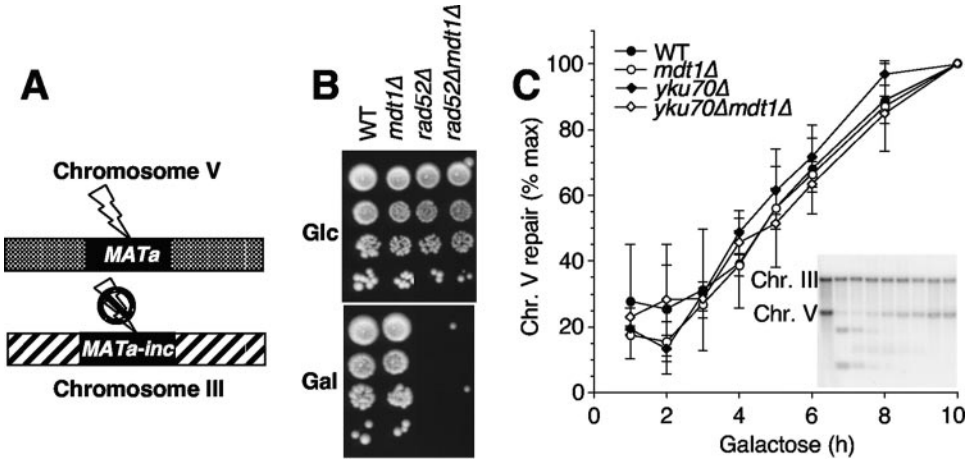

FIG. 5. Response to a single HO endonuclease-induced repairable DSB. (A) Schematic diagram of the assay. *GAL1*-inducible HO cleaves a single site in the genome at an ectopic *MAT***a** locus on chromosome V. HML and HMR are deleted in this strain, and repair by HR depends on an uncleavable *MAT***a**-inc template. (B) Tenfold serial dilutions (from top to bottom) of the indicated strains on glucose where HO is repressed and galactose where HO is expressed. (C) Repair kinetics of the HO-induced DSB in the indicated strains at the indicated times after galactose addition. Results are the averages and ranges of two independent experiments. The insert shows a representative Southern blot of the wild type at 0, 1, 2, 3, 4, 5, 6, 8, and 10 h. The uncleavable chromosome III band serves as a loading control for quantification.

strain that contains 10 HO cleavage sites within a subset of *Ty1* elements in addition to the physiological site at *MAT***a** (34), but *mdt1*Δ also did not lead to noticeably increased HO sensitivity in this system (data not shown) (note that the *MAT***a** HO site is restored by the *HML*/*HMR* repair templates in this strain, and continued *GAL1-HO* expression is therefore toxic even for wild-type cells).

***mdt1*Δ increases the sensitivity of partially recombination-deficient cells to camptothecin-induced protein-blocked DSBs.** Another possible explanation for the discrepancy between the bleomycin epistasis experiments and the HO assays was that although bleomycin and HO both give rise to DSBs, the structures of these DSBs are actually not the same, as enzyme-generated DSBs contain a free 3′-hydroxyl end whereas bleomycin-induced DSBs contain a 3′-phospho-glycolate-blocked end (5). To test if Mdt1 might be specifically required for the repair of blocked drug-induced DSBs as opposed to "clean" endonuclease-generated breaks, we measured the sensitivity of *mdt1*Δ cells to another blocked-end-generating drug, camptothecin, which stabilizes the topoisomerase I-DNA cleavage intermediate and thereby gives rise to replication-dependent 3′-phospho-tyrosyl protein-blocked DSBs (52). Although *mdt1*Δ alone did not impair cell growth in the continuous presence of camptothecin, it markedly increased the camptothecin sensitivity of partially HR-defective *rad51*Δ and *rad55*Δ mutants by >10-fold (Fig. 6A), supporting the hypothesis that Mdt1 may specifically promote recombination efficiency at blocked DNA ends. No such genetic interactions were observed in response to MMS as a structurally unrelated form of DNA damage (Fig. 6B), indicating that *mdt1*Δ indeed acts in a 3′-blocked-end lesion-specific manner.

***mdt1*Δ reduces the efficiency of recombinational telomere maintenance.** To further test the hypothesis that Mdt1 might function to facilitate blocked-end-specific recombination, we sought a system where this could be studied in a drug-free manner, similar to the HO endonuclease assay for "clean" DSBs (Fig. 5). As outlined above, telomeres are natural DSB mimics in that they represent a linear double-stranded DNA end, and they are hidden underneath a protein cap—thus, resembling protein-blocked DSBs—but the recombination machinery has to be able to gain access to them in order to escape cellular senescence in the absence of telomerase. Based on these considerations, and because of the genetic link of *MDT1* to telomere-related functions of KU in the bleomycin response (Fig. 2C), we chose to analyze *mdt1*Δ effects on telomerase-independent telomere maintenance.

To monitor cell senescence, six independent colonies per genotype from freshly dissected spores of a compound heterozygote for the telomerase catalytic protein subunit gene *EST2*/*est2*Δ, *MDT1*/*mdt1*Δ, and *RAD52*/*rad52*Δ were grown in liquid medium for 8 days, with determination of cell densities and dilution to 10^5 cells/ml in 24-hour intervals. Wild-type and *mdt1*Δ cultures grew back to ~10^8 cells/ml after each dilution throughout the experiment (Fig. 7A). *rad52*Δ and *rad52*Δ *mdt1*Δ cultures grew only to ~3.5×10^7 cells/ml after each dilution; however, the generally slower growth rate of *rad52*Δ was stable throughout the experiment and therefore not related to senescence (Fig. 7A). As expected, *est2*Δ cultures showed the typical senescence phenotype with progressively declining cell densities until day 6, followed by detectable survivor formation by day 7 and restoration of proliferation rates to nearly wild-type levels by day 8 (Fig. 7A). *est2*Δ *mdt1*Δ cultures senesced with virtually indistinguishable kinetics from *est2*Δ and formed survivors at the same time, but interestingly, proliferation rates of the double mutant survivors stagnated at a level that was lower even than that of *rad52*Δ mutants (Fig. 7A). Proliferation rates of *est2*Δ and *est2*Δ *mdt1*Δ cultures lacking *RAD52* progressively declined and never recovered (Fig. 7A), confirming that survivor formation in this assay is recombination dependent.

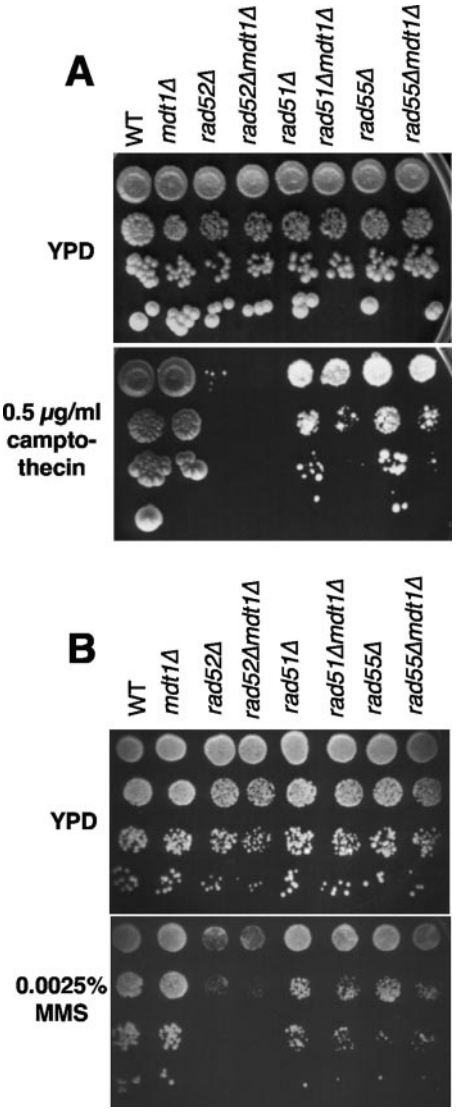

FIG. 6. Camptothecin and MMS sensitivity assays. Tenfold serial dilutions (from top to bottom) of the indicated strains were plated on YPD or YPD containing 0.5 μg/ml camptothecin (A) or 0.0025% MMS (B). Note that *rad55*Δ and *rad55*Δ *mdt1*Δ are both *SML1*.

We also extended this widely used senescence assay (6) by replating a defined number of cells on YPD plates in order to determine their ability to form colonies as a measure of their long-term viability (Fig. 7B). Remarkably, whereas *est2*Δ survivors eventually regained 100% viability, only ~20% of *est2*Δ *mdt1*Δ double mutant survivors were able to form colonies in

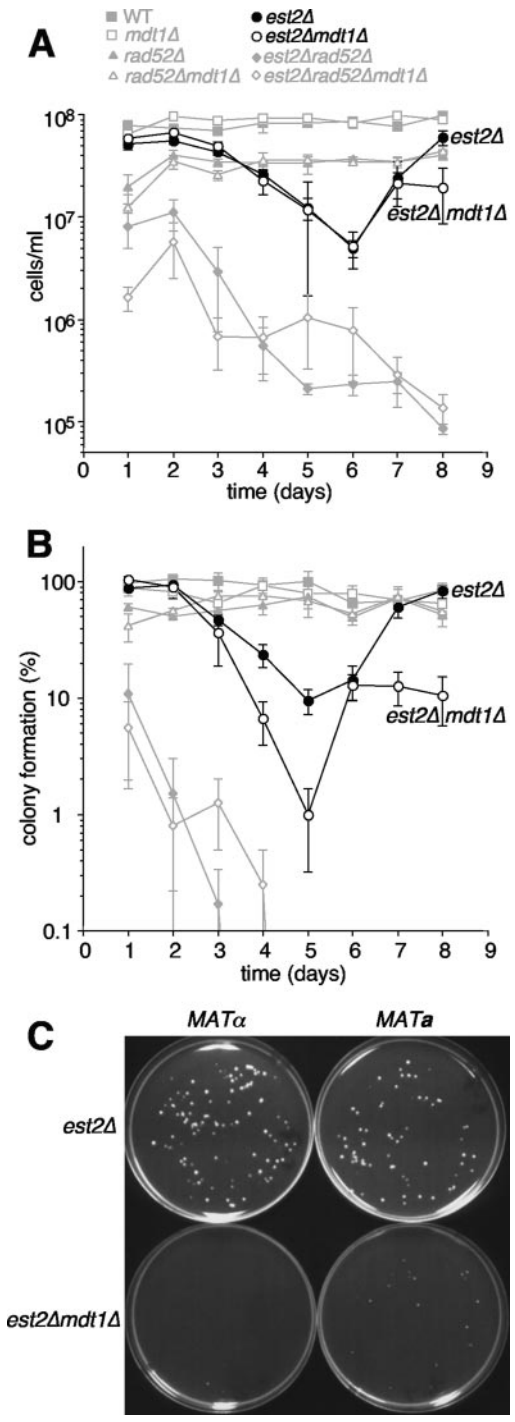

FIG. 7. Senescence assays. (A) Freshly sporulated colonies with the indicated genotypes were transferred to liquid YPD cultures, and at 24-hour intervals cells were counted and cultures diluted to 10^5 cells/ml. Results are the means ± standard errors of six independent clones per genotype. For clarity, only *est2*Δ and *est2*Δ *mdt1*Δ are shown in black, and controls are shown in gray. In this case, all cultures were analyzed in parallel in three control-matched batches staggered by 2 hours to minimize the delay between cell counts and dilutions. (B) Colony-forming ability of the strains shown in panel A. Each day, 100 to 200 cells per culture were plated, and the percent colony formation was assessed 3 to 4 days later. (C) Photograph of 2-day-old plates inoculated with 100 cells of the indicated genotypes after day 7 of the liquid survival assay, sporulated from a separate diploid than shown in panels A and B.

this assay, and this was again recombination dependent (Fig. 7B). Note that in this assay, *mdt1*Δ seemingly accelerated the onset of senescence from loss of *EST2* (Fig. 7B, compare mutants at days 4 and 5), but because formation of visible colonies from senescing cultures depends on survivor formation, this result is likely an indirect consequence of reduced survivor viability in the double mutant.

Qualitatively similar results were obtained in two separate repeat experiments with another seven independent clones per genotype from an unrelated *EST2*/*est2*Δ *MDT1*/*mdt1*Δ sporulation, where *mdt1*Δ consistently reduced the viability of *est2*Δ survivors (data not shown), and this phenotype was independent of the mating type (Fig. 7C). In addition, consistent with lower viability rates, *est2*Δ *mdt1*Δ survivor colonies (note, but not freshly sporulated presenescent colonies [data not shown]) were also smaller than *est2*Δ colonies (Fig. 7C). Altogether, these results indicate that postsenescence survivors are unable to sustain an efficient recombination-based telomere maintenance mechanism in the absence of *MDT1*.

***mdt1*Δ leads to a shift from type II to type I postsenescence survivor formation.** Telomerase-deficient yeast cells form two types of recombination-dependent survivors, type I survivors that are characterized by very short homogenous telomeres and type II survivors that are characterized by very heterogenous and often excessively elongated telomere patterns (6). Type I survivors form more frequently than type II survivors, but the latter proliferate much faster and therefore typically overgrow type I survivors in liquid cultures (6, 60). The simplest explanation for the reduced proliferation rates and viability of *est2*Δ *mdt1*Δ double mutants compared to *est2*Δ, therefore, was that *mdt1*Δ impairs type II survivor formation.

To test this possibility, we randomly chose a single colony from day 8 survivor plates for each of the independent *est2*Δ and *est2*Δ *mdt1*Δ cultures (Fig. 7A and B) for Southern blot analysis of telomere length profiles. Remarkably, whereas all six *est2*Δ survivors had the characteristically heterogenous telomere length pattern of type II survivors, all six *est2*Δ *mdt1*Δ survivors had the typical short and homogenous terminal restriction fragment length pattern of type I survivors (Fig. 8A). Similar results were also obtained in the day 8 liquid cultures of four independent clones per genotype in repeat experiments from a separate sporulation strain (Fig. 8B). In pedigree analyses, 29 of 30 individual survivor colonies from 10 independent *est2*Δ spores had a type II telomere pattern and only 1 out of 30 had a type I pattern (data not shown). In contrast, among 50 survivors from 10 independent *est2*Δ *mdt1*Δ spores, we recovered only 2 type II survivors (and 1 mixed type I/type II clone) (data not shown). As type I survivors can give rise to type II survivors (but not vice versa) (60), we tested if the transition from type I to type II might be delayed in *mdt1*Δ mutants. Four independent *est2*Δ *mdt1*Δ type I survivor colonies were therefore cultured for another 6 days with daily back-dilution to 10^5 cells/ml and daily removal of aliquots for Southern blot analysis, but in all cases the type I telomere pattern was stably maintained throughout the experiment (data not shown). Altogether, these results demonstrate that the absence of *MDT1* leads to a dramatic shift in the mechanism of postsenescence survivor formation in telomerase mutants, from >90% type II to >90% of the less-efficient type I telomere recombination mechanism.

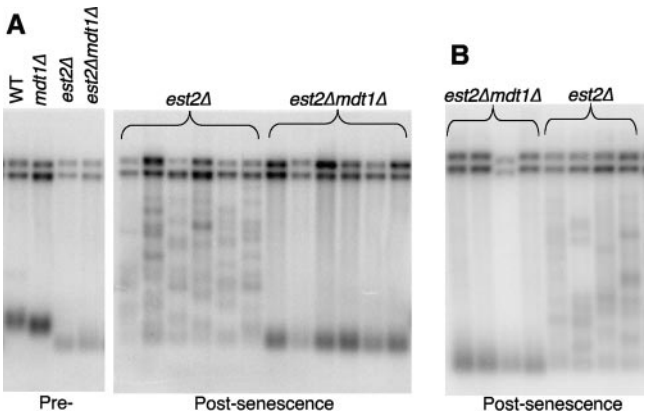

FIG. 8. Telomere Southern blot analyses. (A) XhoI-digested DNA of the indicated presenescent strains (left panel) and six randomly chosen postsenescent *est2*Δ and *est2*Δ *mdt1*Δ day 8 survivor colonies, each representing an independent spore (right panel), were probed with a Y′-probe. (B) XhoI-digested DNA prepared directly from day 8 liquid cultures of four independent spores each derived from a separate diploid strain than shown in panel A were probed with a Y′-probe.

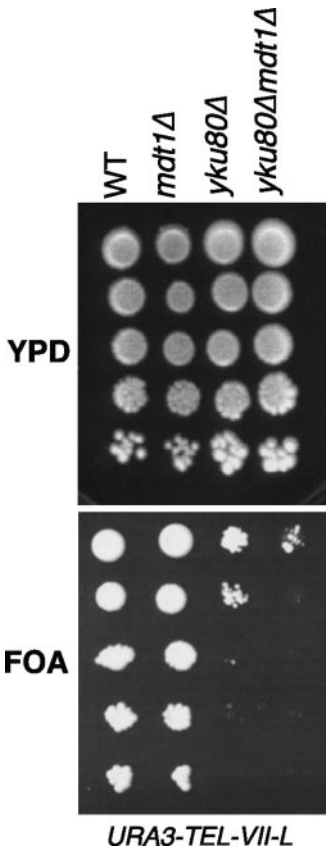

FIG. 9. Subtelomeric silencing assays. Tenfold serial dilutions of the indicated strains were spotted on YPD or FOA plates.

Telomere-related phenotypes of *mdt1*Δ in telomerase-positive cells. It should be noted that the absence of *MDT1* resulted in very subtly shortened telomeres in telomerase-positive cells (Fig. 8A, left panel). Because of this and its synthetic genetic interaction with *cft18*Δ (Fig. 3) that was recently shown to affect telomere anchoring at the nuclear periphery (21), we tested if Mdt1 may have a general role in telomere structural maintenance (independent of cellular senescence) by analyzing its effect on silencing of a subtelomeric *URA3* reporter gene in the left arm of chromosome VII. In this assay, in wild-type cells the *URA3* gene is silenced and cells can grow on plates containing 5-FOA. In contrast to the *yku80*Δ control, which resulted in ~1,000-fold-reduced colony formation on FOA plates, *mdt1*Δ alone did not noticeably impair silencing (Fig. 9). Interestingly, however, *mdt1*Δ increased the silencing defect of *yku80*Δ a further 10-fold (Fig. 9), indicating that Mdt1 seems to contribute to the KU-independent telomere position effect pathway (38).

DISCUSSION

Here we have shown that *mdt1*Δ cells are exquisitely sensitive to bleomycin, in a manner that, based on epistasis with the *rad52*Δ *yku70*Δ double deletion that disables the three most common DSB repair pathways (Fig. 2), is related to a role in the repair of bleomycin-induced DSBs. Likewise, normal onset of Rad53 phosphorylation in response to bleomycin addition but impaired checkpoint recovery after bleomycin removal (Fig. 1D and E) and indirect hyperactivation of the DSB-specific Tel1 kinase (Fig. 1C) in *mdt1*Δ mutants are consistent with a role of Mdt1 in DSB repair. Furthermore, we have directly shown that *mdt1*Δ cells are impaired in their ability to restore broken chromosomes after bleomycin treatment (Fig. 4). In addition to the *RAD52*-dependent HR pathway and the KU-dependent NHEJ and chromosome healing pathways, yeast contains a poorly characterized fourth DSB repair pathway, the microhomology-mediated end-joining pathway. However, a characteristic feature of microhomology-mediated end-joining mutations is that they render *rad52*Δ *yku70*Δ more sensitive to DSBs (37), and the fact that *mdt1*Δ does not do this demonstrates that its bleomycin sensitivity is unrelated to the alternative end-joining pathway. Instead, epistasis with the *rad52*Δ *yku70*Δ double deletion but synergism with the respective single deletions indicates that Mdt1 acts in the repair of bleomycin-induced DSBs in a more general facilitator role by regulating the efficiency of both the HR and the KU pathway. Such a facilitator function would also be consistent with the finding that *mdt1*Δ alone does not affect camptothecin tolerance but that it further increases sensitivity when the HR pathway is partially impaired by deletion of *RAD51* or *RAD55* (Fig. 6), and most importantly, that it leads to a dramatic shift to the less-efficient type I recombination pathway of telomerase-independent telomere maintenance (Fig. 7 and 8).

A surprising finding was that *mdt1*Δ leads to a very severe hypersensitivity to bleomycin-induced DSBs but not (apart from the relatively modest synthetic camptothecin effects) to enzyme-generated DSBs (Fig. 5) or to a range of other DNA-damaging agents (Fig. 6B and data not shown) that give rise to DSBs at least as a fraction of their lesion spectrum. However, this seemingly remarkable "agent-specific" DSB sensitivity is consistent with the notion that not all DSBs are alike and that even subtle differences in precise DSB structures may lead to distinct repair outcomes. For example, in an extreme case, it has recently been demonstrated that DSB repair pathways for

3′-phospho-tyrosyl-topoisomerase I-blocked DSBs are differentially affected depending on whether the Top1 cleavage intermediate is stabilized as a consequence of the *top1-T722A* mutation or as a result of camptothecin treatment (52). With regard to bleomycin sensitivity, our results are in a way a mirror image of recent findings from the Symington laboratory that Mre11 nuclease deficiency differentially affects the repair of the more complex multisite-damaged ionizing radiation-induced DSBs but not bleomycin-induced 3-phospho-glycolate-blocked DSBs (34). The specific bleomycin hypersensitivity of *mdt1*Δ is also remarkably similar to the *smc5-33* mutation that, in contrast to other *smc5* alleles, seems to selectively affect the response to bleomycin but not to several other DNA-damaging agents (9). It should be noted that we also tested *mdt1*Δ for genetic interactions with the *smc5-31* and *smc5-33* alleles, and in both cases *mdt1*Δ led to increased bleomycin sensitivity (data not shown), indicating that although *mdt1*Δ and *smc5-33* share a remarkably specific bleomycin hypersensitivity, they seem to be doing so as part of separate pathways. Remarkably, *mdt1*Δ entirely abolished the restoration of bleomycin-damaged chromosomes, apparently even without the appearance of repair intermediates (Fig. 4), indicating that Mdt1 is required for a very early repair stage.

A common link between bleomycin- and camptothecin-induced DSBs and telomeres is that they all represent some form of blocked DSB. Furthermore, bleomycin and camptothecin specifically block the 3′ end of DSBs in the form of 3′-phospho-glycolate- or 3′-phospho-tyrosyl protein-blocked ends, respectively. *MDT1* does not seem to be required for sporulation (12), during which the Spo11 protein remains covalently bound to the 5′ end of the DSBs it generates (44). It is therefore tempting to speculate that Mdt1 is specifically required for the repair of 3′- but not 5′-blocked DSBs. But how would telomeres fit this structural consideration? Interestingly, telomeres end in G-rich 3′-single-stranded tails, which in yeast are bound by the telomere-specific ssDNA-binding proteins Cdc13, Stn1, and Ten1, part of whose function it is to block inadvertent recombination between chromosome ends (16). In analogy to the bleomycin- and camptothecin-induced lesions, telomeres might thus be considered as 3′-phospho-G-tail protein-blocked DSBs that in some way have to become unblocked in an *MDT1*-dependent manner for efficient recombination to occur when it is required to maintain viability in the absence of telomerase.

For some reason *mdt1*Δ was not detected in a recent genome-wide high-throughput screen for bleomycin-hypersensitive mutants in the S288C background (1), although in our hands it is also bleomycin sensitive in this background (albeit at higher doses and longer treatment times than used here for W303 [data not shown]). A total of >200 genes were identified in that screen, most of which are unlikely to function in DSB repair (1). In contrast, many fewer factors have so far been identified that, similarly to Mdt1, are specifically required for the efficient type II telomere maintenance pathway, and the vast majority of these are clearly involved in general aspects of DNA recombination, for example, Rad50 (6), Rad59 (6), Sgs1 (22), Top3 (65), Exo1 (40), Clb2/Cdk kinase activity (15), and in diploid cells, mating type heterozygosity (36). Additional factors that promote type II survivor formation but are probably not directly linked to the HR process include the Mec1 and Tel1 checkpoint kinases (66) and the Def1 subunit of the transcription-coupled repair protein Rad26 (7). Remarkably, similarly to Mdt1, Def1 also contains an extensive C-terminal SQ/TQ cluster domain as a potential Mec1/Tel1 phosphorylation target (64), and given their similar survivor phenotypes it would be interesting to see whether Mec1/Tel1-dependent phosphorylation of these clusters indeed contributes to alternative telomere maintenance pathways. In contrast to genes such as *SGS1* and *RAD59* that are essential for type II recombination (6, 22), but similarly to *rad50*Δ (6), *mdt1*Δ did not entirely eliminate type II survivors in liquid senescence assays, and we were also able to recover type II survivors in plate restreak assays (data not shown). As mentioned above, in telomerase mutants without additional recombination defects, type I survivors are generally generated more frequently (and therefore dominate in less-competitive solid-phase senescence assays), but type II survivors grow much faster and therefore end up overgrowing competing type I cells in liquid cultures (6, 60). Our results that *mdt1*Δ *est2*Δ cells are in principle able to generate type II survivors, but that these do not dominate liquid cultures even after extended growth periods, therefore suggest that Mdt1 is probably more important for the efficiency of the type II recombination process than the transition from the type I to the type II survival pathway. It should be noted that *MDT1* has similar synergistic interactions with *RAD50* (required for type II survival) and *RAD51* (required for type I) in the bleomycin response (Fig. 2B), indicating that recombinational repair of 3′-phospho-glycolate-blocked ends does not simply mimic the type II pathway of recombinational telomere maintenance.

Mdt1 is likely to exert its functions described here as part of a protein complex, but very little is currently known about Mdt1 (see the Saccharomyces Genome Database [www.yeastgenome.org]), and it is therefore hard to speculate what this complex might be and by what molecular mechanisms it may regulate recombination efficiency. Interestingly, in a high-throughput protein affinity copurification screen, Mdt1 was found to interact with the INO80 component Rvb2 (14), but despite this proposed direct interaction, the synthetic interaction between *mdt1*Δ and the nonessential INO80 component *ARP5* (Fig. 3A) indicates that Mdt1 and INO80 act in the bleomycin response as part of separate pathways. The remarkably similar dose-response curves as single mutants coupled with the dramatic synthetic bleomycin hypersensitivity phenotype between *mdt1*Δ and *ctf18*Δ (Fig. 3A) indicate that Mdt1 acts in a pathway that collaborates extensively with the Ctf18-containing cohesin-loading clamp. Moreover, the *ctf18*Δ *mdt1*Δ synthetic sickness phenotype under basal conditions (Fig. 3B) indicates that the interaction between these pathways is also relevant for the proper processing of physiological DNA lesions. Interestingly, Ctf18 has recently also been linked to telomere functions by regulating their proper positioning in the nuclear periphery (21), a process that is important for the efficient recombinational repair of subtelomeric DSBs (62), but it is currently not known if Ctf18 affects postsenescence recombinational telomere maintenance in a similar manner. Nevertheless, the results presented here have identified Mdt1 as a new recombination facilitator that is important for the efficiency of alternative telomere maintenance and the efficiency of the repair of blocked DSBs generated by a subset of

chemotherapeutic agents, and they provide a basis for future studies of the precise mechanisms involved. As Mdt1 is structurally related to a human protein, ASCIZ (41), it will be interesting to see if similar mechanisms are conserved in metazoans.

ACKNOWLEDGMENTS

We thank Nora Tenis and Tricia Lo Liang for assistance with blot analyses; Trevor Lithgow and his laboratory for access to the Singer yeast dissection microscope; Brenda Andrews, Lorraine Symington, Greg Cost, Rodney Rothstein, and Jim Haber for yeast strains; and Ana Traven and Monique Smeets for comments on the manuscript.

This work was supported by grants from the National Health and Medical Research Council of Australia to J.H. and a grant from the Harold and Cora Brennen Benevolent Trust for purchase of PFGE equipment.

REFERENCES

1. **Aouida, M., N. Page, A. Leduc, M. Peter, and D. Ramotar.** 2004. A genome-wide screen in Saccharomyces cerevisiae reveals altered transport as a mechanism of resistance to the anticancer drug bleomycin. Cancer Res. **64:**1102–1109.
2. **Aylon, Y., B. Liefshitz, and M. Kupiec.** 2004. The CDK regulates repair of double-strand breaks by homologous recombination during the cell cycle. EMBO J. **23:**4868–4875.
3. **Boulton, S. J., and S. P. Jackson.** 1998. Components of the Ku-dependent non-homologous end-joining pathway are involved in telomeric length maintenance and telomeric silencing. EMBO J. **17:**1819–1828.
4. **Chan, S. W., and E. H. Blackburn.** 2003. Telomerase and ATM/Tel1p protect telomeres from nonhomologous end joining. Mol. Cell **11:**1379–1387.
5. **Chen, J., and J. Stubbe.** 2005. Bleomycins: towards better therapeutics. Nat. Rev. Cancer **5:**102–112.
6. **Chen, Q., A. Ijpma, and C. W. Greider.** 2001. Two survivor pathways that allow growth in the absence of telomerase are generated by distinct telomere recombination events. Mol. Cell. Biol. **21:**1819–1827.
7. **Chen, Y. B., C. P. Yang, R. X. Li, R. Zeng, and J. Q. Zhou.** 2005. Def1p is involved in telomere maintenance in budding yeast. J. Biol. Chem. **280:**24784–24791.
8. **Corda, Y., S. E. Lee, S. Guillot, A. Walther, J. Sollier, A. Arbel-Eden, J. E. Haber, and V. Geli.** 2005. Inactivation of Ku-mediated end joining suppresses *mec1*Δ lethality by depleting the ribonucleotide reductase inhibitor Sml1 through a pathway controlled by Tel1 kinase and the Mre11 complex. Mol. Cell. Biol. **25:**10652–10664.
9. **Cost, G. J., and N. R. Cozzarelli.** 2006. Smc5p promotes faithful chromosome transmission and DNA repair in Saccharomyces cerevisiae. Genetics **172:**2185–2200.
10. **de Lange, T.** 2005. Shelterin: the protein complex that shapes and safeguards human telomeres. Genes Dev. **19:**2100–2110.
11. **Enomoto, S., L. Glowczewski, and J. Berman.** 2002. MEC3, MEC1, and DDC2 are essential components of a telomere checkpoint pathway required for cell cycle arrest during senescence in Saccharomyces cerevisiae. Mol. Biol. Cell **13:**2626–2638.
12. **Enyenihi, A. H., and W. S. Saunders.** 2003. Large-scale functional genomic analysis of sporulation and meiosis in Saccharomyces cerevisiae. Genetics **163:**47–54.
13. **Fasching, C. L., K. Bower, and R. R. Reddel.** 2005. Telomerase-independent telomere length maintenance in the absence of alternative lengthening of telomeres-associated promyelocytic leukemia bodies. Cancer Res. **65:**2722–2729.
14. **Gavin, A. C., M. Bosche, R. Krause, P. Grandi, M. Marzioch, A. Bauer, J. Schultz, J. M. Rick, A. M. Michon, C. M. Cruciat, M. Remor, C. Hofert, M. Schelder, M. Brajenovic, H. Ruffner, A. Merino, K. Klein, M. Hudak, D. Dickson, T. Rudi, V. Gnau, A. Bauch, S. Bastuck, B. Huhse, C. Leutwein, M. A. Heurtier, R. R. Copley, A. Edelmann, E. Querfurth, V. Rybin, G. Drewes, M. Raida, T. Bouwmeester, P. Bork, B. Seraphin, B. Kuster, G. Neubauer, and G. Superti-Furga.** 2002. Functional organization of the yeast proteome by systematic analysis of protein complexes. Nature **415:**141–147.
15. **Grandin, N., and M. Charbonneau.** 2003. Mitotic cyclins regulate telomeric recombination in telomerase-deficient yeast cells. Mol. Cell. Biol. **23:**9162–9177.
16. **Grandin, N., C. Damon, and M. Charbonneau.** 2001. Cdc13 prevents telomere uncapping and Rad50-dependent homologous recombination. EMBO J. **20:**6127–6139.
17. **Groff-Vindman, C., A. J. Cesare, S. Natarajan, J. D. Griffith, and M. J. McEachern.** 2005. Recombination at long mutant telomeres produces tiny single- and double-stranded telomeric circles. Mol. Cell. Biol. **25:**4406–4412.
18. **Haber, J. E.** 2000. Partners and pathways repairing a double-strand break. Trends Genet. **16:**259–264.
19. **Hammet, A., B. L. Pike, K. I. Mitchelhill, T. Teh, B. Kobe, C. M. House, B. E. Kemp, and J. Heierhorst.** 2000. FHA domain boundaries of the Dun1p and Rad53p cell cycle checkpoint kinases. FEBS Lett. **471:**141–146.
20. **Hanna, J. S., E. S. Kroll, V. Lundblad, and F. A. Spencer.** 2001. *Saccharomyces cerevisiae* CTF18 and CTF4 are required for sister chromatid cohesion. Mol. Cell. Biol. **21:**3144–3158.
21. **Hiraga, S., E. D. Robertson, and A. D. Donaldson.** 2006. The Ctf18 RFC-like complex positions yeast telomeres but does not specify their replication time. EMBO J. **25:**1505–1514.
22. **Huang, P., F. E. Pryde, D. Lester, R. L. Maddison, R. H. Borts, I. D. Hickson, and E. J. Louis.** 2001. SGS1 is required for telomere elongation in the absence of telomerase. Curr. Biol. **11:**125–129.
23. **Ira, G., A. Malkova, G. Liberi, M. Foiani, and J. E. Haber.** 2003. Srs2 and Sgs1-Top3 suppress crossovers during double-strand break repair in yeast. Cell **115:**401–411.
24. **Ira, G., A. Pellicioli, A. Balijja, X. Wang, S. Fiorani, W. Carotenuto, G. Liberi, D. Bressan, L. Wan, N. M. Hollingsworth, J. E. Haber, and M. Foiani.** 2004. DNA end resection, homologous recombination and DNA damage checkpoint activation require CDK1. Nature **431:**1011–1017.
25. **Keogh, M. C., J. A. Kim, M. Downey, J. Fillingham, D. Chowdhury, J. C. Harrison, M. Onishi, N. Datta, S. Galicia, A. Emili, J. Lieberman, X. Shen, S. Buratowski, J. E. Haber, D. Durocher, J. F. Greenblatt, and N. J. Krogan.** 2006. A phosphatase complex that dephosphorylates gammaH2AX regulates DNA damage checkpoint recovery. Nature **439:**497–501.
26. **Krogan, N. J., M. H. Lam, J. Fillingham, M. C. Keogh, M. Gebbia, J. Li, N. Datta, G. Cagney, S. Buratowski, A. Emili, and J. F. Greenblatt.** 2004. Proteasome involvement in the repair of DNA double-strand breaks. Mol. Cell **16:**1027–1034.
27. **Krogh, B. O., and L. S. Symington.** 2004. Recombination proteins in yeast. Annu. Rev. Genet. **38:**233–271.
28. **Larrivee, M., and R. J. Wellinger.** 2006. Telomerase- and capping-independent yeast survivors with alternate telomere states. Nat. Cell Biol. **8:**741–747.
29. **Le, S., J. K. Moore, J. E. Haber, and C. W. Greider.** 1999. RAD50 and RAD51 define two pathways that collaborate to maintain telomeres in the absence of telomerase. Genetics **152:**143–152.
30. **Lee, S. J., M. F. Schwartz, J. K. Duong, and D. F. Stern.** 2003. Rad53 phosphorylation site clusters are important for Rad53 regulation and signaling. Mol. Cell. Biol. **23:**6300–6314.
31. **Leroy, C., S. E. Lee, M. B. Vaze, F. Ochsenbien, R. Guerois, J. E. Haber, and M. C. Marsolier-Kergoat.** 2003. PP2C phosphatases Ptc2 and Ptc3 are required for DNA checkpoint inactivation after a double-strand break. Mol. Cell **11:**827–835.
32. **Lin, C. Y., H. H. Chang, K. J. Wu, S. F. Tseng, C. C. Lin, C. P. Lin, and S. C. Teng.** 2005. Extrachromosomal telomeric circles contribute to Rad52-, Rad50-, and polymerase delta-mediated telomere-telomere recombination in *Saccharomyces cerevisiae*. Eukaryot. Cell **4:**327–336.
33. **Lisby, M., J. H. Barlow, R. C. Burgess, and R. Rothstein.** 2004. Choreography of the DNA damage response: spatiotemporal relationships among checkpoint and repair proteins. Cell **118:**699–713.
34. **Llorente, B., and L. S. Symington.** 2004. The Mre11 nuclease is not required for 5′ to 3′ resection at multiple HO-induced double-strand breaks. Mol. Cell. Biol. **24:**9682–9694.
35. **Lombard, D. B., K. F. Chua, R. Mostoslavsky, S. Franco, M. Gostissa, and F. W. Alt.** 2005. DNA repair, genome stability, and aging. Cell **120:**497–512.
36. **Lowell, J. E., A. I. Roughton, V. Lundblad, and L. Pillus.** 2003. Telomerase-independent proliferation is influenced by cell type in Saccharomyces cerevisiae. Genetics **164:**909–921.
37. **Ma, J. L., E. M. Kim, J. E. Haber, and S. E. Lee.** 2003. Yeast Mre11 and Rad1 proteins define a Ku-independent mechanism to repair double-strand breaks lacking overlapping end sequences. Mol. Cell. Biol. **23:**8820–8828.
38. **Maillet, L., F. Gaden, V. Brevet, G. Fourel, S. G. Martin, K. Dubrana, S. M. Gasser, and E. Gilson.** 2001. Ku-deficient yeast strains exhibit alternative states of silencing competence. EMBO Rep. **2:**203–210.
39. **Mantiero, D., M. Clerici, G. Lucchini, and M. P. Longhese.** 2007. Dual role for Saccharomyces cerevisiae Tel1 in the checkpoint response to double-strand breaks. EMBO Rep. **8:**380–387.
40. **Maringele, L., and D. Lydall.** 2004. EXO1 plays a role in generating type I and type II survivors in budding yeast. Genetics **166:**1641–1649.
41. **McNees, C. J., L. A. Conlan, N. Tenis, and J. Heierhorst.** 2005. ASCIZ regulates lesion-specific Rad51 focus formation and apoptosis after methylating DNA damage. EMBO J. **24:**2447–2457.
42. **Morrison, A. J., J. Highland, N. J. Krogan, A. Arbel-Eden, J. F. Greenblatt, J. E. Haber, and X. Shen.** 2004. INO80 and gamma-H2AX interaction links ATP-dependent chromatin remodeling to DNA damage repair. Cell **119:**767–775.
43. **Muntoni, A., and R. R. Reddel.** 2005. The first molecular details of ALT in human tumor cells. Hum. Mol. Genet. **14**(Spec. 2)**:**R191–R196.
44. **Neale, M. J., J. Pan, and S. Keeney.** 2005. Endonucleolytic processing of covalent protein-linked DNA double-strand breaks. Nature **436:**1053–1057.
45. **Pan, X., P. Ye, D. S. Yuan, X. Wang, J. S. Bader, and J. D. Boeke.** 2006. A DNA integrity network in the yeast Saccharomyces cerevisiae. Cell **124:**1069–1081.

46. **Pellicioli, A., S. E. Lee, C. Lucca, M. Foiani, and J. E. Haber.** 2001. Regulation of Saccharomyces Rad53 checkpoint kinase during adaptation from DNA damage-induced G_2/M arrest. Mol. Cell **7:**293–300.
47. **Pennaneach, V., C. D. Putnam, and R. D. Kolodner.** 2006. Chromosome healing by de novo telomere addition in Saccharomyces cerevisiae. Mol. Microbiol. **59:**1357–1368.
48. **Pike, B. L., A. Hammet, and J. Heierhorst.** 2001. Role of the N-terminal forkhead-associated domain in the cell cycle checkpoint function of the Rad53 kinase. J. Biol. Chem. **276:**14019–14026.
49. **Pike, B. L., N. Tenis, and J. Heierhorst.** 2004. Rad53 kinase activation-independent replication checkpoint function of the N-terminal forkhead-associated (FHA1) domain. J. Biol. Chem. **279:**39636–39644.
50. **Pike, B. L., S. Yongkiettrakul, M. D. Tsai, and J. Heierhorst.** 2003. Diverse but overlapping functions of the two forkhead-associated (FHA) domains in Rad53 checkpoint kinase activation. J. Biol. Chem. **278:**30421–30424.
51. **Pike, B. L., S. Yongkiettrakul, M. D. Tsai, and J. Heierhorst.** 2004. Mdt1, a novel Rad53 FHA1 domain-interacting protein, modulates DNA damage tolerance and G_2/M cell cycle progression in *Saccharomyces cerevisiae*. Mol. Cell. Biol. **24:**2779–2788.
52. **Pouliot, J. J., C. A. Robertson, and H. A. Nash.** 2001. Pathways for repair of topoisomerase I covalent complexes in Saccharomyces cerevisiae. Genes Cells **6:**677–687.
53. **Ramotar, D., and H. Wang.** 2003. Protective mechanisms against the anti-tumor agent bleomycin: lessons from Saccharomyces cerevisiae. Curr. Genet. **43:**213–224.
54. **Richardson, C., and M. Jasin.** 2000. Recombination between two chromosomes: implications for genomic integrity in mammalian cells. Cold Spring Harbor Symp. Quant. Biol. **65:**553–560.
55. **Sanchez, Y., B. A. Desany, W. J. Jones, Q. Liu, B. Wang, and S. J. Elledge.** 1996. Regulation of RAD53 by the ATM-like kinases MEC1 and TEL1 in yeast cell cycle checkpoint pathways. Science **271:**357–360.
56. **Shim, E. Y., J. L. Ma, J. H. Oum, Y. Yanez, and S. E. Lee.** 2005. The yeast chromatin remodeler RSC complex facilitates end joining repair of DNA double-strand breaks. Mol. Cell. Biol. **25:**3934–3944.
57. **Stellwagen, A. E., Z. W. Haimberger, J. R. Veatch, and D. E. Gottschling.** 2003. Ku interacts with telomerase RNA to promote telomere addition at native and broken chromosome ends. Genes Dev. **17:**2384–2395.
58. **Takata, H., Y. Kanoh, N. Gunge, K. Shirahige, and A. Matsuura.** 2004. Reciprocal association of the budding yeast ATM-related proteins Tel1 and Mec1 with telomeres in vivo. Mol. Cell **14:**515–522.
59. **Tam, A. T., B. L. Pike, A. Hammet, and J. Heierhorst.** 2007. Telomere-related functions of yeast KU in the repair of bleomycin-induced DNA damage. Biochem. Biophys. Res. Commun. **357:**800–803.
60. **Teng, S. C., and V. A. Zakian.** 1999. Telomere-telomere recombination is an efficient bypass pathway for telomere maintenance in *Saccharomyces cerevisiae*. Mol. Cell. Biol. **19:**8083–8093.
61. **Teo, S. H., and S. P. Jackson.** 1997. Identification of Saccharomyces cerevisiae DNA ligase IV: involvement in DNA double-strand break repair. EMBO J. **16:**4788–4795.
62. **Therizols, P., C. Fairhead, G. G. Cabal, A. Genovesio, J. C. Olivo-Marin, B. Dujon, and E. Fabre.** 2006. Telomere tethering at the nuclear periphery is essential for efficient DNA double strand break repair in subtelomeric region. J. Cell Biol. **172:**189–199.
63. **Tong, A. H., G. Lesage, G. D. Bader, H. Ding, H. Xu, X. Xin, J. Young, G. F. Berriz, R. L. Brost, M. Chang, Y. Chen, X. Cheng, G. Chua, H. Friesen, D. S. Goldberg, J. Haynes, C. Humphries, G. He, S. Hussein, L. Ke, N. Krogan, Z. Li, J. N. Levinson, H. Lu, P. Menard, C. Munyana, A. B. Parsons, O. Ryan, R. Tonikian, T. Roberts, A. M. Sdicu, J. Shapiro, B. Sheikh, B. Suter, S. L. Wong, L. V. Zhang, H. Zhu, C. G. Burd, S. Munro, C. Sander, J. Rine, J. Greenblatt, M. Peter, A. Bretscher, G. Bell, F. P. Roth, G. W. Brown, B. Andrews, H. Bussey, and C. Boone.** 2004. Global mapping of the yeast genetic interaction network. Science **303:**808–813.
64. **Traven, A., and J. Heierhorst.** 2005. SQ/TQ cluster domains: concentrated ATM/ATR kinase phosphorylation site regions in DNA-damage-response proteins. BioEssays **27:**297–307.
65. **Tsai, H. J., W. H. Huang, T. K. Li, Y. L. Tsai, K. J. Wu, S. F. Tseng, and S. C. Teng.** 2006. Involvement of topoisomerase III in telomere-telomere recombination. J. Biol. Chem. **281:**13717–13723.
66. **Tsai, Y. L., S. F. Tseng, S. H. Chang, C. C. Lin, and S. C. Teng.** 2002. Involvement of replicative polymerases, Tel1p, Mec1p, Cdc13p, and the Ku complex in telomere-telomere recombination. Mol. Cell. Biol. **22:**5679–5687.
67. **Unal, E., A. Arbel-Eden, U. Sattler, R. Shroff, M. Lichten, J. E. Haber, and D. Koshland.** 2004. DNA damage response pathway uses histone modification to assemble a double-strand break-specific cohesin domain. Mol. Cell **16:**991–1002.
68. **Usui, T., H. Ogawa, and J. H. Petrini.** 2001. A DNA damage response pathway controlled by Tel1 and the Mre11 complex. Mol. Cell **7:**1255–1266.
69. **Valencia, M., M. Bentele, M. B. Vaze, G. Herrmann, E. Kraus, S. E. Lee, P. Schar, and J. E. Haber.** 2001. NEJ1 controls non-homologous end joining in Saccharomyces cerevisiae. Nature **414:**666–669.
70. **Valencia-Burton, M., M. Oki, J. Johnson, T. A. Seier, R. Kamakaka, and J. E. Haber.** 2006. Different mating-type-regulated genes affect the DNA repair defects of Saccharomyces RAD51, RAD52 and RAD55 mutants. Genetics **174:**41–55.
71. **van Attikum, H., O. Fritsch, B. Hohn, and S. M. Gasser.** 2004. Recruitment of the INO80 complex by H2A phosphorylation links ATP-dependent chromatin remodeling with DNA double-strand break repair. Cell **119:**777–788.
72. **Vega, L. R., M. K. Mateyak, and V. A. Zakian.** 2003. Getting to the end: telomerase access in yeast and humans. Nat. Rev. Mol. Cell Biol. **4:**948–959.
73. **Wilson, T. E., U. Grawunder, and M. R. Lieber.** 1997. Yeast DNA ligase IV mediates non-homologous DNA end joining. Nature **388:**495–498.
74. **Zhao, X., E. G. Muller, and R. Rothstein.** 1998. A suppressor of two essential checkpoint genes identifies a novel protein that negatively affects dNTP pools. Mol. Cell **2:**329–340.
75. **Zhou, B. B., and S. J. Elledge.** 2000. The DNA damage response: putting checkpoints in perspective. Nature **408:**433–439.